Linking Fabrication Information Modeling and Finite Cell Method for simulating the behavior of additively manufactured building components

Oguz Oztoprak, Martin Slepicka, András László Aninger, Stefan Kollmannsberger, Ernst Rank and André Borrmann
Technical University of Munich, Arcisstr. 21, 80333, Munich, Germany
oguz.oztoprak@tum.de

Additive manufacturing (AM) in construction presents challenges due to the complexity of component design. Fabrication Information Modelling (FIM) streamlines digital design and manufacturing by partially automating the process, but evaluating component functionality requires numerical simulation tools. We propose integrating the Finite Cell Method (FCM) into the FIM workflow, as it handles complex geometries with a high degree of automation. We develop an approach to represent the digital print path models as lightweight, 3D geometrical models, seamlessly integrating them into FCM analysis. Boundary conditions are specified based on the additional information from the FIM model, with relevant surfaces automatically generated and extracted. We demonstrate this workflow through a variant study on structural wall elements with internal structures, highlighting the FIM and FCM integration in design and analysis cycles. Integrating simulation capabilities into FIM provides valuable insights during early design stages, extending the digital chain from design to fabrication information to simulation-enhanced variant studies for AM products.

Introduction

Additive manufacturing (AM) in construction is a fast-growing research area due to its potential for increased flexibility, automated processes, and improved design. With AM processes, components can be customized for specific uses, such as incorporating gaps or taking advantage of unique shapes. However, this flexibility also leads to challenges in designing these components, which can be difficult to handle using traditional digital methods. Integrating individual functions adds additional complexity that needs tailored design, increasing the effort for design, verification, and validation.

Fabrication Information Modelling (FIM), a recent development in the construction industry, allows for the creation of essential fabrication information based on BIM and geometric patterns in a partially automated manner (Slepicka et al., 2022). Currently, FIM is focussing on extrusion-based AM methods using robotic arms. Despite some limitations, FIM can significantly speed up digital design and manufacturing processes by facilitating communication between design and production. However, applying printing patterns in FIM follows specific rules, and determining the performance of a component, such as its mechanical or thermal properties, requires physical testing or numerical simulation. To efficiently evaluate and compare different AM component variations created using FIM, it is essential to integrate numerical simulation tools into the FIM workflow.

The analysis of the structural and thermal performance of extrusion-based 3D-printed building components has been the subject of numerous simulation-based studies. Alkhalidi and Hatuqay (2020) have studied, based on the finite element method (FEM), the thermal performance of real-life sized 3D printed planar wall with a fixed 4 cm square nozzle. They conclude that a U-value as low as 0.15 W/m^2 was achievable based on a distinct printing material and wall configuration with cavities. Wang et al. (2020) employed the discrete element method (DEM) to simulate the mechanical behavior of various lightweight 3DPC samples with hollow internal

structures. Van Zijl et al. (2021) and Poologanathan et al. (2021) examined the thermal performance of numerous wall configurations with macrostructural cavity arrangements.

In this contribution, we present an approach to integrate the simulation capabilities of the Finite Cell Method (FCM) with FIM to create a fully streamlined digital manufacturing and design process for extrusion-based AM. The FCM is an extension of the classical finite elements approach that can handle a wide range of geometric models with a high degree of automation. The digital model of the print paths represented by means of the Industry Foundation Classes (IFC) data model is incorporated to construct a lightweight, 3D geometrical model that can be seamlessly integrated into the FCM analysis. The geometric model is constructed by sweeping a section along the print path, which enables it to easily accommodate different cross-sections of the filament. The resulting watertight 3D geometrical model is used for mechanical and thermal analysis. To demonstrate the capabilities of the workflow, a variant study on parametrically designed wall elements with internal structures is conducted. This involves analyzing the thermal and mechanical performance of distinct wall variants with a focus on minimizing engineering effort. Since analyzing multiple variants requires several simulations to characterize their thermal and mechanical responses, integrating FIM with an automated simulation framework can significantly simplify the design and analysis iterations.

Background

1.1 FIM parametric path planning

While in traditional construction methods, components are usually built completely solid, additive manufacturing can be used to design the interior of the component. For example, cavities can be created in the component through clever design to save weight or to positively influence the component properties, such as the thermal insulation capacity of a wall. It should be noted, however, that structural integrity and support must be carefully considered when customizing voids in 3D-printed components, especially if the component is load bearing. In this context, a strategy based on parametric patterns can be useful for designing the internal cavities in 3D-printed components, as it enables a more flexible and efficient design process. By using parametric modelling tools, designers can quickly test and iterate different patterns and configurations of the internal cavities to find optimized solutions. Through simple variation of the patterns and the corresponding parameters, several model variants can be generated quickly, which can later be compared and evaluated using simulations.

For additive manufacturing, a 3D geometry including the desired cavities is usually created first and then cut into individual 2D slices (slicing). Area-filling curves are then generated for these 2D surfaces, often subdivided into a contour zone and a so-called "hatching" zone, to form the printing path. The contour zone ensures shape accuracy, while the hatching zone is used for time and material-efficient printing.

A different strategy is used with FIM when focused on extrusion-based concrete printing. 3D printing with concrete presents a particular challenge due to the conflicting material properties required for additive manufacturing. The material must be *pumpable*, *extrudable*, but also *buildable*. In other words, it must be flowable and deformable, but once it leaves the extruder nozzle, it must be able to immediately support its own weight and that of the subsequent layers. Another issue for 3D printing is the fact that concrete is a thixotropic material, which means that it loses plasticity when subjected to vibrations. All these factors have a significant influence on how the printing process must be carried out, and thus also on the path planning. To avoid vibrations and to prevent clogging (pumpability/extrudability), the print path should preferably be uninterrupted and smooth as possible (C2-continuous), and overlaps should be avoided as

far as possible. Accordingly, the print path for each print layer should be a simple closed curve, which is rarely the case in conventional path planning for 3D printing (Slepicka et al., 2022). For this reason, FIM proceeds as follows:

The component is first designed in the building model (BIM) without the cavities. The geometry is then extracted as a B-Rep, which in turn is cut into individual 2D contour curves. Finally, the selected pattern is fitted to this contour curve utilizing different design parameters to generate the print path. The pattern-based path planning thus indirectly generates the intended cavities.

As a choice for design patterns, simple recurring geometries, such as zigzag, sinusoidal or cellular patterns, are applicable. The patterns can be identical for each layer, or they can be varied per layer to create closed chambers or other complex 3D structures. With a suitable pattern choice, material consumption can be reduced, and the strength-to-weight ratio, as well as thermal or acoustic insulation, can be improved. However, it is not possible to give a general answer to the exact effect or even feasibility of these design patterns. For an estimation of the structural stability and other performance values, it is generally recommended to perform a numerical simulation.

1.2 From print paths to numerical analysis

The print paths can be used to construct lightweight geometric models on which efficient numerical analysis is performed. Building such a volumetric model based on procedural geometry is discussed next.

Procedural geometric modelling

Procedural modelling describes geometry through a sequence of operations, including face-to-solid operations (rotation, extrusion, lofting) and Constructive Solid Geometry (CSG). CSG is a 3D modelling approach based on the combination of a set of primitives, such as cylinders, spheres, etc. Union, intersection, and difference are the basic Boolean operations to combine various primitive objects, resulting in potentially complex geometries. The final object can be represented as a binary CSG tree. Within the context of extrusion-based AM, print paths can be used to construct primitive volumetric objects by extruding the filament cross-section along the path. The volumetric model of the entire structure is then obtained by taking the union of the swept primitives across all layers. The resulting geometric model has a lightweight structure and a low memory footprint as each swept object is described by a curve in 3D and a corresponding cross-section (Rank et al., 2012).

Swept primitives naturally form closed 3D objects that are watertight. Consequently, geometric models consisting of CSG primitives generally demand less manual pre-processing than classical Boundary Representation (B-Rep) schemes, making them a good fit for streamlined processes (Wassermann et al., 2017).

A shortcoming of CSG-based geometric models is that only an indirect access to the surface description is available, and therefore intermediate steps must be taken to approximate the surfaces, e.g., by using the marching cubes algorithm (Lorensen and Cline, 1987). Explicit surface description might be needed for visualization and application of boundary conditions in the case of embedded simulation methods (Düster et al., 2017).

Finite Cell Method

The Finite Cell Method (FCM) is an extended variation of the conventional finite element method, incorporating high-order finite elements in the context of an immersed boundary approach. The fundamental concept of FCM is illustrated in Fig. 1. The actual domain, Ω_{phy}, is embedded in a fictitious domain, Ω_{fic}, so that the combined domain, $\Omega_{\cup}$, forms a simple shape

that can be trivially meshed. An indicator function α is used to distinguish between the physical and the fictitious domain, where it is defined as:

$$\alpha = \begin{cases} 1 & \forall x \in \Omega_{\text{phy}} \\ 10^{-q} & \forall x \in \Omega_{\text{fic}}. \end{cases} \tag{1}$$

A suitably small α (typically, $q = 8$ to 10 is deemed sufficient) ensures that the incorporation of the embedding domain does not introduce substantial errors. Consequently, the difficulty of creating an appropriate mesh, which might require significant manual effort in certain instances, is replaced by recovery of the original physical domain during accurate numerical integration. In this process, integration techniques like the space-tree subdivision (e.g., octree subdivision in 3D) can be employed for precise integration (see Hubrich et al., 2017).

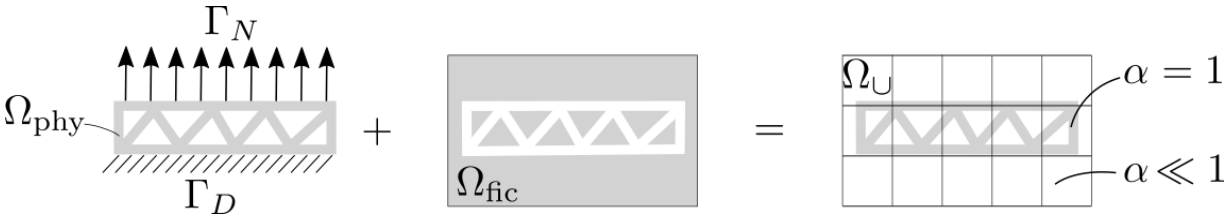

Figure 1: Illustration of the Finite Cell Method, following Düster et al. (2008). The physical domain Ω_{phy} is extended by the fictitious domain Ω_{fic}, where their union $\Omega_\cup$ can be trivially meshed. The scaling factor α serves to penalize the effect of the fictitious domain.

The bilinear form of a steady state linear heat conduction problem, for example, can be formulated as:

$$a(v,T) = \int_{\Omega_\cup} \nabla v \cdot \alpha\, \mathbf{K} \cdot \nabla T \; d\Omega\,, \tag{2}$$

where v is the test function, T is a function representing the temperature and $\mathbf{K}$ is the thermal conductivity tensor. The corresponding right-hand side functional can be written as:

$$f(v) = \int_{\Omega_\cup} \alpha\, v\; \bar{s}\; d\Omega + \int_{\Gamma_N} v\; \bar{q}\; d\Gamma, \tag{3}$$

$$T = \bar{T} \qquad \forall \boldsymbol{x} \in \Gamma_D, \tag{4}$$

where $\bar{s}$ represents a distributed heat source, $\bar{q}$ is the prescribed heat flux on the surface Γ_N and $\bar{T}$ is the prescribed temperature on Γ_D. Since the finite cell discretization does not conform to the boundary of the physical domain Ω_{phy}, additional care is required when imposing the boundary conditions in Eq. (3). Homogeneous Neumann boundary conditions require no special treatment, like classical FEM. However, non-homogeneous Neumann boundary conditions can be enforced by computing the boundary integral term in Eq. (3) using an explicit surface discretization of Γ_N. Conversely, Dirichlet boundary conditions in Eq. (4) can be imposed weakly by augmenting the weak form with additional constraints on Γ_D. In this contribution, the penalty approach will be utilized to weakly impose Dirichlet boundary conditions (Düster et.al, 2017). For both the Neumann and Dirichlet boundary conditions, a separate surface discretization is needed to evaluate the boundary integrals. The generation of such a surface

mesh, in general, can require substantial engineering effort. Streamlining the surface mesh generation for the application of the boundary conditions is a key aspect that is further investigated within the context of 3D-printed wall elements.

Generation of surface discretization

Thermal analysis on wall elements requires temperature boundary conditions on the inner and outer surfaces of the wall. Therefore, the relevant discretised surfaces must be available prior to an FCM analysis. However, the CSG-based volumetric model does not explicitly represent the boundaries of the wall element. A suitable surface mesh, on which the boundary conditions can be applied, is generated by approximating the implicitly defined surfaces using polygonization techniques (e.g., marching cubes algorithm by Lorensen and Cline, 1987) within oriented bounding cuboids. The bounding cuboids are constructed based on the tangent planes, which are tangent to the surface of the wall element, as illustrated in Fig. 2. The tangent planes are translated (by a distance based on the nozzle size) towards the negative normal direction such that the original and translated planes form a cuboid when the corresponding points are connected, the resulting cuboid is shown in light grey in Fig 2, right.

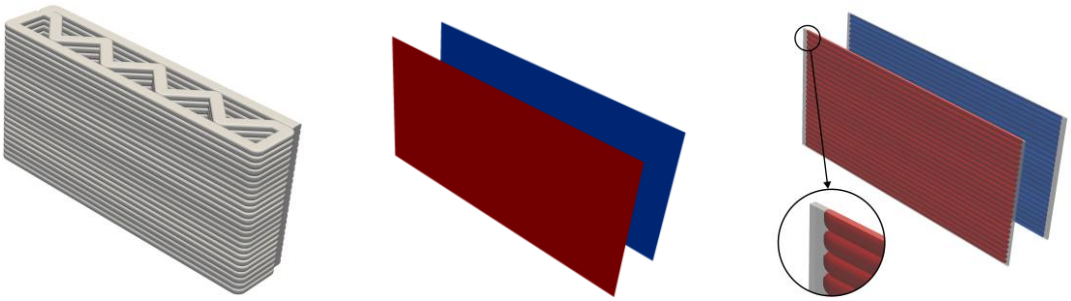

Figure 2: An example wall element (left), the inner and outer tangent planes from FIM (middle), and the generated surface meshes inside the oriented bounding boxes (right).

Computation of the U-value

The U-value is a measure of the rate of heat transfer through a building element, where a lower U-value indicates better thermal insulation and reduced heat loss, while a higher U-value reveals inferior insulation. It has a unit of W/m^2K and can be computed as follows (ISO 6946:2017):

$$U = \frac{Q}{A \cdot \Delta T}, \tag{5}$$

where Q is the total heat flux through the surface, A is the surface area, and ΔT is the temperature difference between the inside and outside of the wall element. In this contribution, we compute the total heat flux Q through the inner and outer surfaces of the wall (D'Angella et al. 2022) and calculate the U-value following Eq. (5).

Methodology

The following section describes, on the one hand, the workflow to derive manufacturing information from a BIM model using FIM and, on the other hand, how this data is subsequently processed for simulation purposes. For the extraction of the BIM data and the subsequent generation of the manufacturing information, a script was developed for the BIM-capable CAD software Autodesk Revit using the graphical programming interface Dynamo. First, components for which manufacturing information is to be generated are selected individually

from a BIM model. The component itself, its inner sides, and the position of the AM system must be selected. The boundary representation of the selected component can then be broken down topologically with the specified interior sides, providing the individual boundary surfaces sorted by their orientation (top, bottom, interior, exterior). Using the lateral surfaces (interior, exterior) and the process and pattern parameters (see Fig. 3), the corresponding printing path for the component is then generated layer by layer in the form of a composite curve of basic geometries such as lines, arcs, and splines. All further steps that may follow, such as the generation of a speed profile for the robot and the extruder, are not considered in this work.

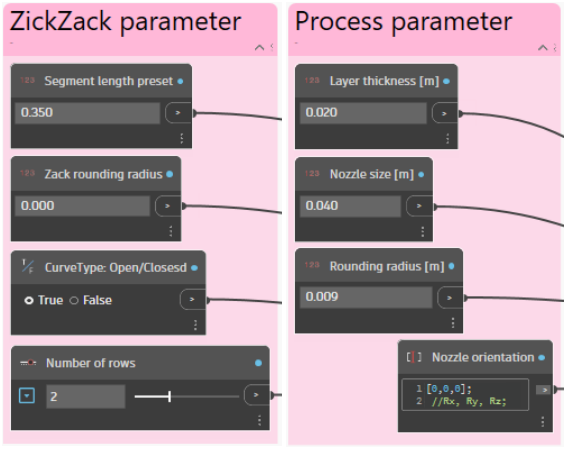

Figure 3: Dynamo input masks for specifying process and pattern parameters.

The generated data (printing path and sorted outer surfaces) are then saved in IFC data format for each component (cf. Slepicka et al., 2022) and provided in this form for simulation with the in-house FCM framework, AdhoC++. A freely available FCM implementation is provided by Zander et al., 2014. With a plugin (Aninger et al., 2022) for AdhoC++, the path information available in the individual IFC files can be read and converted into a simulation model using CSG-based geometric modeling (see Section 2.2).

Numerical studies

1.3 Validation

The approach for performing numerical analysis on proposed geometric models is validated for 3D steady state heat transfer analysis. The robustness of linear elastic analysis on similar geometric models is demonstrated in Wassermann et al. (2017). Given the scarcity of experimental data for the thermal performance of large-scale extruded wall elements, validation is undertaken through comparison with existing published research. To this end, a partial wall element model from Alkhalidi and Hatuqay (2020) is realized based on the print paths from the FIM. The reference wall model from Alkhalidi and Hatuqay (2020), the print paths from the FIM, and the boundary representation of the CSG-based geometric model is shown in Fig. 4. In contrast to the reference model, which considers a perfect square nozzle, the geometric model in this contribution assumes a rectangular filament cross-section with rounded corners (Fig. 4, right).

A steady state 3D heat transfer analysis is conducted where a temperature difference of $\Delta T = 20\,K$ is imposed as a Dirichlet boundary condition on the inner ($293\,K$) and outer ($273\,K$) surface of the wall. The thermal conductivity of concrete is taken as $0.367\,W/m\,°K$, corresponding to the first concrete mixture in the reference publications. Furthermore, the convection and the radiation of the unventilated air cavities inside the wall are modelled by an effective thermal conductivity approach based on ISO 6946 (ISO 6946:2017). An FCM mesh resolution of $92 \times 21 \times 44$ is chosen for the analysis, where the polynomial degree is $p = 4$, the octree integration depth is $d = 5$, the alpha FCM is $\alpha = 10^{-10}$ and the penalty factor used for weak imposition of the boundary conditions is 10^{12} (see Düster et al. (2017) for the detailed definition of these parameters).

A U-value of 1.81 $W/m^2\,K$ is obtained from the 3D heat transfer simulation. The resulting temperature field and the heat flux density are shown in Fig. 5.

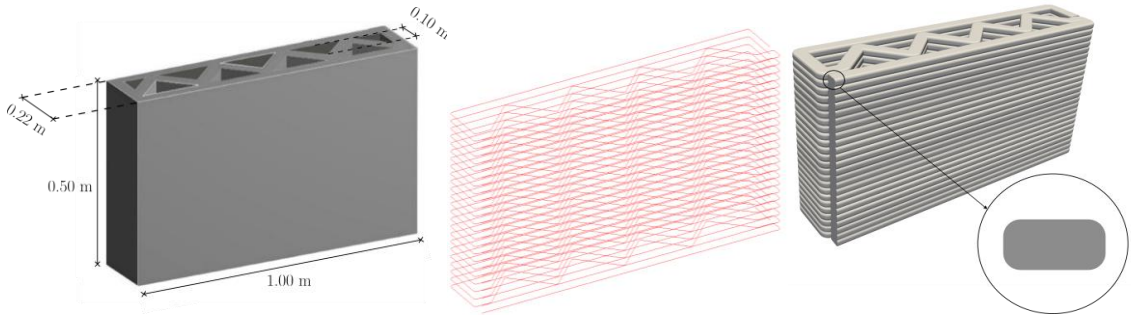

Figure 4: The reference wall element geometry (left), the designed print paths (middle), and the surface reconstruction of the CSG-based volumetric model with the filament cross-section (right).

The result displays an excellent agreement with the reference U-values computed by Alkhalidi and Hatuqay (2020) using Ansys, who obtained U-values of 1.80 W/m^2K and 1.87 $W/m^2\ K$ for temperature differences of $20\ K$ and $40\ K$, respectively. Additionally, the 3D heat transfer analysis (Abaqus) by Pologanathan et al. (2021) also computed the U-value of the reference model to be approximately 1.80 $W/m^2\ K$ for a temperature difference of $40\ K$.

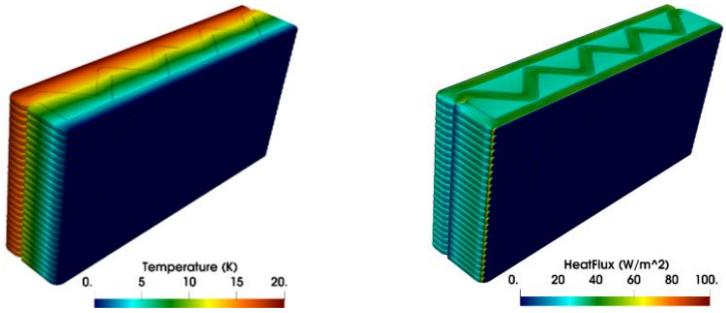

Figure 5: The temperature field (left) and the heat flux distribution (right) from the validation study, visualized on the reconstructed boundary surface.

1.4 Variant Study

In order to demonstrate the usefulness of the workflow proposed in this study, a variant study is carried out below. For this purpose, a BIM building model consisting of a single room was created. The background of this investigation is the problem that thermal bridges can occur at building corners. Without proper insulation, building corners have an increased heat flow which can lead to condensation and moisture build-up if the spot becomes too cold (Abdykalykov et al., 2021). In the following variant study, the effect of different corner designs and different AM patterns on the heat flow is demonstrated.

Room model

The room model for this variant study was designed so that each corner is slightly different (cf. Fig. 6). In addition to the regularly designed corner, there were three other designs incorporated that are assumed to have better heat flow, the chamfered corner, which splits the 90° corner into two less problematic 135° corners, the filleted corner, which increases the inner surface, and the circular "corner", which is a more extreme variant of the filleted corner. The four distinct corners are to be investigated for thermal and mechanical performance.

Infill variants

In addition to the four different corner variations, three different infill patterns and two wall thicknesses are also investigated in this study (see Fig. 6b).

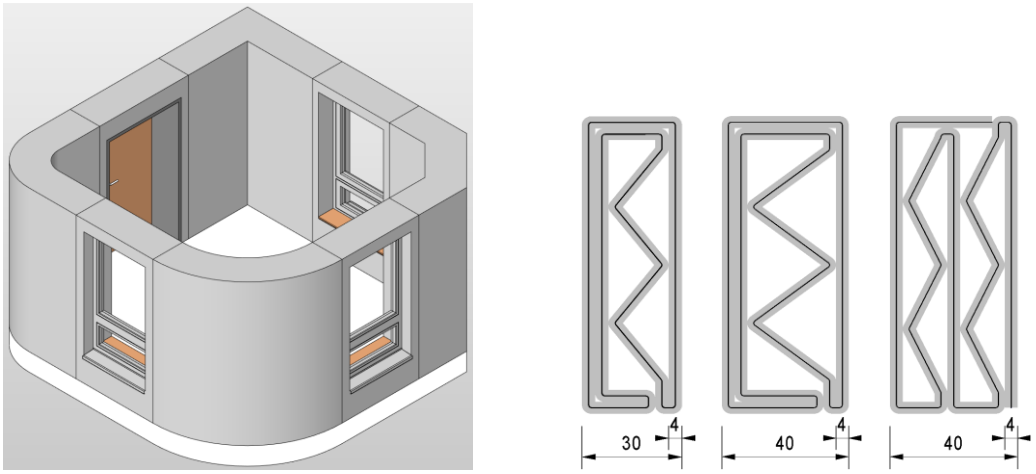

(a) (b)

Figure 6: a) Room model used for numerical study of different corner variants: regular (top), chamfered (right), circular (bottom), and rounded (left). b) Different zigzag variants: V1 (left), V2 (middle) and V3 (right).

Numerical results

The four corner variants are analysed considering three different wall interior alternatives, as shown in Fig. 6b, utilizing the FCM with procedural geometric models (Section 2). The U-values resulting from steady state 3D heat transfer analysis on the variants are depicted in Fig. 8. A temperature difference of $\Delta T = 20\ K$ is imposed between the inner and the outer surfaces of the walls, and the thermal conductivity of concrete is taken as 0.367 $W/\ m\ °K$. An effective thermal conductivity approach based on ISO 6946 is employed to model the convection and the radiation of unventilated air cavities inside the wall, analogous to the validation study. To accurately capture the geometric details of the walls, ~2.5 million degrees of freedom are used, where the polynomial degree is $p = 5$, the octree integration depth is $d = 5$, the alpha FCM is $\alpha = 10^{-10}$ and the penalty value used for weak imposition of the boundary conditions is 10^{12}. The corresponding heat flux distributions are illustrated in Fig. 10. The visualizations in Fig. 10 are generated by mapping the results from the analysis onto the 3D surface reconstructions of the procedural geometric models, following the marching cubes algorithm (Lorensen and Cline, 1987).

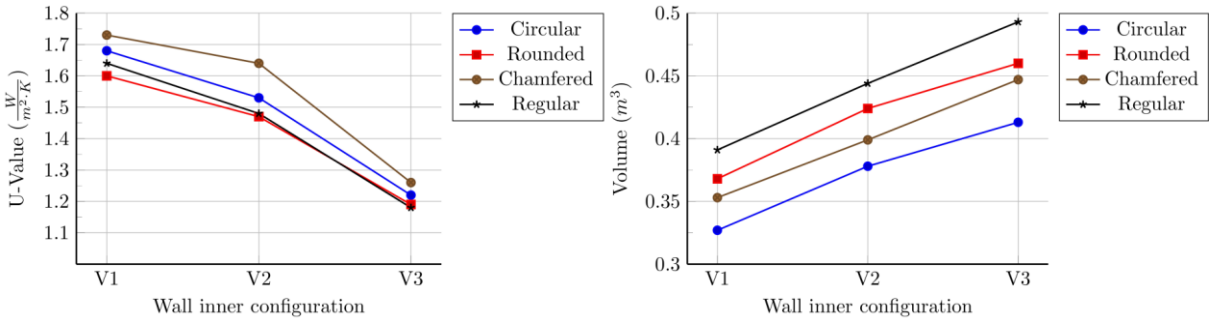

Figure 8: U-value results obtained for different configurations (left) and the material volume of the variants in m^3 (right)

In general, the double zigzag configuration with 0.4 m wall thickness, denoted as V3, provides a visible improvement in the U-value compared to its V1 and V2 variants. For example, the V3 variant of the circular wall exhibits approximately 20% better insulation properties (Fig. 8, left)

while using approximately 10% more material (Fig. 8, right). It is important to note that experimental validation is necessary to verify the resulting U-values.

Using an identical workflow for a structural simulation, the necessary loadbearing capacity of all construction variants is verified. Details are omitted due to the space restrictions.

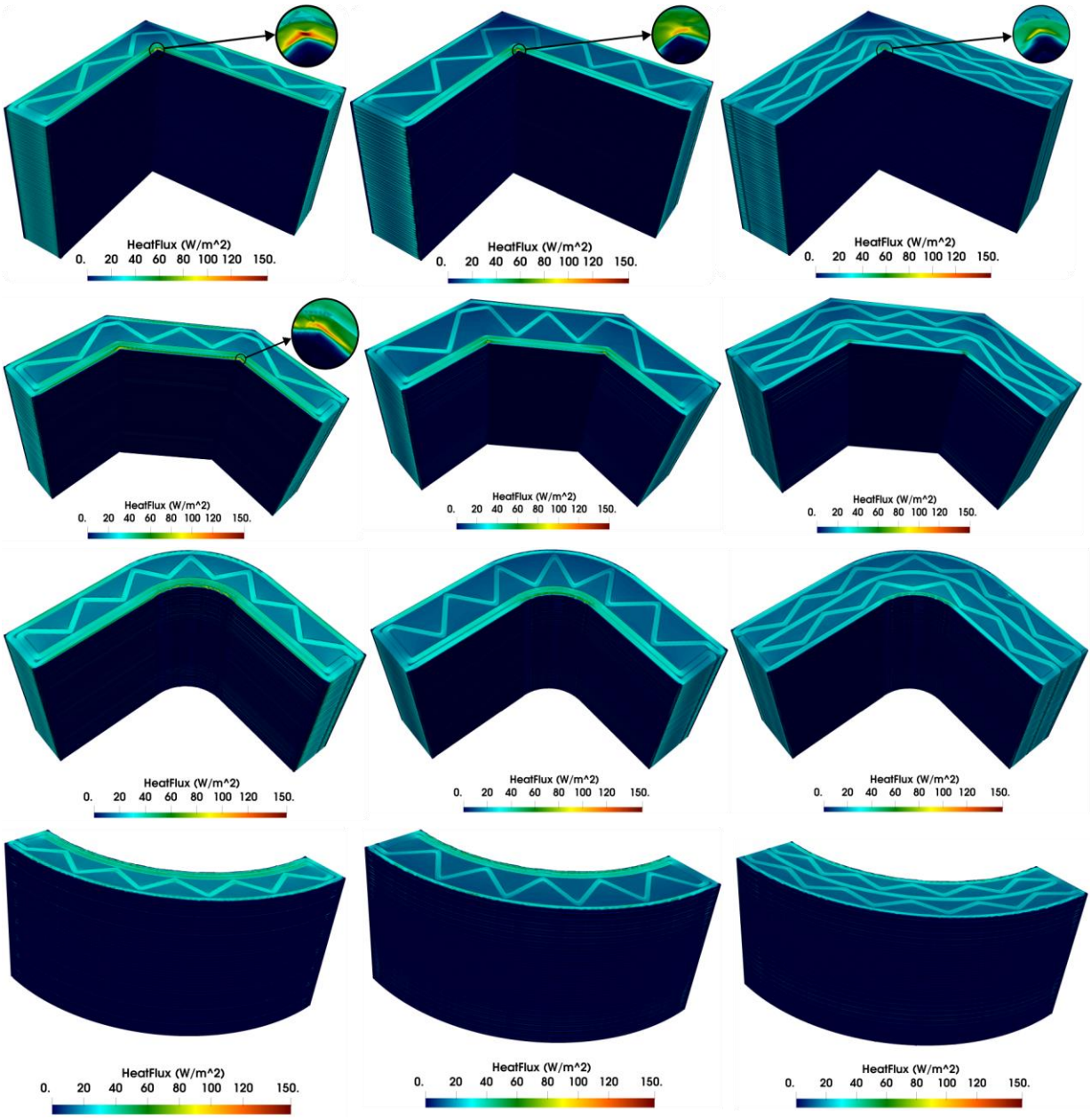

Figure 10: The heat flux magnitude of the variants, configurations with fluxes higher than $100\ W/m^2$ are depicted with an additional zoom view.

Conclusions

In conclusion, this study presents a unified approach to streamline the digital manufacturing and design process for extrusion-based additive manufactured products by integrating the Finite Cell Method (FCM) with Fabrication Information Modeling (FIM). This integration results in a highly automated workflow that simplifies the design and analysis iterations required for

evaluating and comparing distinct component variants. The FCM's ability to seamlessly handle geometric models of complex AM products, in combination with the capabilities of FIM, allows for efficient assessment of mechanical and thermal performance. The CSG-based implicit models provide an inherently watertight geometric representation, avoiding "dirty geometries" which cause numerous problems in transferring a geometric model to a model valid for computational mechanical analysis (Wassermann et al., 2019). Moreover, the proposed geometric model is sufficiently flexible to handle various filament cross-sections and print paths. The application of this approach to parametrically designed wall elements demonstrates its potential to reduce the manual effort needed from design to analysis. Future research may focus on further enhancing the automation of the integrated FIM-FCM workflow, introducing capabilities to represent the *as-built* geometry (e.g., imperfect print paths and filament sections), as well as extending its applicability to AM products with Functionally Graded Materials (FGM).

Acknowledgments

The research presented is part of the Transregio 277 'Additive Manufacturing in Construction – The Challenge of Large Scale', funded by the Deutsche Forschungsgemeinschaft (DFG, German Research Foundation) – project number 414265976 – TRR 277.

References

Wassermann, B., et al. (2017). From Geometric Design to Numerical Analysis: A Direct Approach Using the Finite Cell Method on Constructive Solid Geometry. Com. & Math. with App., https://doi.org/10.1016/j.camwa.2017.01.027

Düster, A., et al. (2008). The Finite Cell Method for Three-Dimensional Problems of Solid Mechanics. Comp. Meth. in App. Mech. and Eng. doi.org/10.1016/j.cma.2008.02.036

Zander, N., et al. (2014). FCMLab: A finite cell research toolbox for MATLAB. Adv. in Eng. Soft., 74, https://doi.org/10.1016/j.advengsoft.2014.04.004

Aninger, András László (2022). From Fabrication Information Models to Simulation Models. TUM. https://publications.cms.bgu.tum.de/theses/2022_Aninger_FromFIMtoSimulationModels.pdf.

Pologanathan, K., et al. (2021). Energy Performance of 3D-Printed Concrete Walls: A Numerical Study. Buildings 11, https://doi.org/10.3390/buildings11100432.

Wang, L., et al. (2020). Mechanical behaviors of 3D printed lightweight concrete structure with hollow section. https://doi.org/10.1007/s43452-020-00017-1

Alkhalidi, A. and Hatuqay, D. (2020). Energy efficient 3D printed buildings: Material and techniques selection worldwide study. J. of Build. Eng. https://doi.org/10.1016/j.jobe.2020.101286

Van Zijl, G., et al. (2021). Computational assessment of thermal performance of 3D printed concrete wall structures with cavities. Jour. of Building Eng. 41, https://doi.org/10.1016/j.jobe.2021.102431

ISO/TC 163/SC 2 (2022). 'ISO 6946:2017 Building components and building elements — Thermal resistance and thermal transmittance — Calculation methods', https://www.iso.org/standard/65708.html

Lorensen, W.E., Cline, H.E. (1987). Marching Cubes: A high resolution 3D surface construction algorithm. Computer Graphics 21. doi.org/10.1145/37402.37422

Düster, A., Rank, E., Szabó, B. (2017). The p -Version of the Finite Element and Finite Cell Methods, in: Stein, E., de Borst, R., Hughes, T.J.R. (Eds.), Encyclopedia of Computational Mechanics 2nd Edition. John Wiley & Sons, https://doi.org/10.1002/9781119176817.ecm2003g

D'Angella, D., et al. (2022). An accurate strategy for computing reaction forces and fluxes on trimmed locally refined meshes. J. of Mech. https://doi.org/10.1093/jom/ufac006

Abdykalykov, A., et al. (2021). Building wall corner structures, its microclimate and seismic resistance. In E3S Web of Conferences (Vol. 263). http://dx.doi.org/10.1051/e3sconf/202126304051

Slepicka, M., Vilgertshofer, S., and Borrmann, A. (2022). Fabrication information modeling: interfacing building information modeling with digital fabrication. Construction Robotics, 6(2), 87-99. https://doi.org/10.1007/s41693-022-00075-2

Rank, E., et al. (2012) Geometric modeling, isogeometric analysis and the finite cell method. Com. Met. in Ap. Mech. and Eng., doi.org/10.1016/j.cma.2012.05.022

Hubrich, S., et al. (2017). Numerical integration of discontinuous functions: moment fitting and smart octree. C. M. https://doi.org/10.1007/s00466-017-1441-0

Wassermann, B., et al. (2019). Integrating CAD and numerical analysis: 'Dirty geometry' handling using the Finite Cell Method, Comp. Methods in Appl. Mech. and Eng., https://doi.org/10.1016/j.cma.2019.04.017